CANCER

Analysis of *ESR1* mutation in circulating tumor DNA demonstrates evolution during therapy for metastatic breast cancer

Gaia Schiavon,[1,2]* Sarah Hrebien,[1] Isaac Garcia-Murillas,[1] Rosalind J. Cutts,[1] Alex Pearson,[1] Noelia Tarazona,[1] Kerry Fenwick,[1] Iwanka Kozarewa,[1] Elena Lopez-Knowles,[1] Ricardo Ribas,[1] Ashutosh Nerurkar,[2] Peter Osin,[2] Sarat Chandarlapaty,[3] Lesley-Ann Martin,[1] Mitch Dowsett,[1,2] Ian E. Smith,[1,2] Nicholas C. Turner[1,2†]

Acquired *ESR1* mutations are a major mechanism of resistance to aromatase inhibitors (AIs). We developed ultra high–sensitivity multiplex digital polymerase chain reaction assays for *ESR1* mutations in circulating tumor DNA (ctDNA) and investigated the clinical relevance and origin of *ESR1* mutations in 171 women with advanced breast cancer. *ESR1* mutation status in ctDNA showed high concordance with contemporaneous tumor biopsies and was accurately assessed in samples shipped at room temperature in preservative tubes. *ESR1* mutations were found exclusively in estrogen receptor–positive breast cancer patients previously exposed to AI. Patients with *ESR1* mutations had a substantially shorter progression-free survival on subsequent AI-based therapy [hazard ratio, 3.1; 95% confidence interval (CI), 1.9 to 23.1; $P = 0.0041$]. *ESR1* mutation prevalence differed markedly between patients who were first exposed to AI during the adjuvant and metastatic settings [5.8% (3 of 52) versus 36.4% (16 of 44), respectively; $P = 0.0002$]. In an independent cohort, *ESR1* mutations were identified in 0% (0 of 32; 95% CI, 0 to 10.9) tumor biopsies taken after progression on adjuvant AI. In a patient with serial sampling, *ESR1* mutation was selected during metastatic AI therapy to become the dominant clone in the cancer. *ESR1* mutations can be robustly identified with ctDNA analysis and predict for resistance to subsequent AI therapy. *ESR1* mutations are rarely acquired during adjuvant AI but are commonly selected by therapy for metastatic disease, providing evidence that mechanisms of resistance to targeted therapy may be substantially different between the treatment of micrometastatic and overt metastatic cancer.

INTRODUCTION

Cancer evolution and progression are driven by a sequence of somatic genetic and nongenetic alterations resulting in more favorable tumor cell growth and survival. Cancer genetic evolution is subject to intrinsic influences such as the tumor microenvironment, as well as extrinsic pressures such as drug therapy (*1*). The clinical pattern of "acquired" resistance may, in many circumstances, represent outgrowth of resistant clones, which may have originally been present in the cancer at low frequency as a result of intratumoral genetic heterogeneity (*2*, *3*), but grow out under the selective pressure of targeted therapy (*1*). For example, *HER2* amplification is acquired in about 2 to 5% of metastatic breast cancers that were originally *HER2*-nonamplified (*4*). *MET* amplification may be selected out as a mechanism of resistance to epidermal growth factor receptor (EGFR) inhibitor therapy in non–small cell lung cancer (*2*), with the underlying biology behind selection of genetic events, at least in part, reflecting intratumoral heterogeneity and clonal selection.

With the potential of tumor genetics to evolve through treatment, repeat sampling of a tumor would be required to optimally guide therapy because the mechanism of resistance may not be evident in analyses of the tumor before treatment. Yet, serial biopsies of recurrent, metastatic cancer would be invasive, risky, and unacceptable to many patients (*5*). Tumor-derived DNA is found in the plasma of patients with recurrent cancer, and high-depth analysis of circulating tumor DNA (ctDNA) presents a noninvasive way of analyzing tumor genetics and "acquisition" of selected genetic events throughout the course of treatment (*6*, *7*).

About 75% of breast cancers express the estrogen receptor (ER), with hormone therapies being the mainstay of treatment for this group of patients. Hormone resistance is frequent in the treatment of early breast cancer and inevitable in metastatic breast cancer. Recently, mutations in the ER gene (*ESR1*) have been described in advanced breast cancers that had been exposed to previous therapy with aromatase inhibitors (AIs) (*8*–*11*), drugs that suppress estrogen in postmenopausal women through inhibition of androgen aromatization. *ESR1* mutations are only rarely detectable in primary breast cancer and are only found at appreciable frequency after the development of hormone resistance (*11*, *12*). Most of the *ESR1* mutations occur in a hotspot region within the ligand-binding domain (LBD) of ER, altering amino acid 536, 537, or 538 in helix 12 (p.Leu536Arg, p.Tyr537Ser, p.Tyr537Asn, p.Tyr537Cys, and p.Asp538Gly) (*8*–*11*). Functional studies of these LBD *ESR1* mutations demonstrated that they constitutively activate the ER in a ligand-independent fashion (*9*). Hence, cancers with these *ESR1* mutations would be predicted to be resistant to AIs and ovarian suppression in premenopausal women because these therapies work by depriving ligand. In contrast, in vitro and in vivo, LBD *ESR1* mutations retain limited sensitivity to tamoxifen and fulvestrant (a selective ER modulator and a selective ER down-regulator, respectively) (*8*–*11*).

[1]The Breast Cancer Now Research Centre, The Institute of Cancer Research, London SW3 6JB, UK. [2]Breast Unit, Royal Marsden Hospital, Fulham Road, London SW3 6JJ, UK. [3]Department of Medicine, Memorial Sloan Kettering Cancer Center, New York, NY 10065, USA.
*Present address: Translational Science, Oncology iMed, AstraZeneca, Cambridge CB4 0WG, UK.
†Corresponding author. E-mail: nicholas.turner@icr.ac.uk

Previous studies of *ESR1* mutations have been limited to patients with metastatic tumor biopsies and two small studies that have used plasma digital polymerase chain reaction (PCR) (*13*) and plasma amplicon sequencing (*14*) to detect *ESR1* mutations in plasma of patients with metastatic breast cancer. Here, we used ctDNA analysis to study a large, unbiased series of consecutive patients with advanced breast cancer to determine whether these mutations can be detected noninvasively and to examine the potential clinical importance and origin of *ESR1* mutations.

RESULTS

ESR1 mutations are detected in ctDNA of women with ER-positive breast cancer

To investigate whether *ESR1* mutations could be identified in the ctDNA, we recruited a cohort of 171 women with advanced breast cancer (table S1), all of whom had plasma samples taken at the time of disease progression, because ctDNA can become undetectable in patients responding to therapy. We developed ultrahigh-sensitivity multiplex digital PCR assays for *ESR1* LBD mutations and used these to assess for *ESR1* mutations in plasma (Fig. 1A and table S2). To validate ctDNA assessment of *ESR1* mutations, a subset of 31 women had a tumor biopsy contemporaneous to the plasma sample, and there was 97% agreement between tumor DNA and ctDNA analysis [Fig. 1B; $\kappa = 0.84$; 95% confidence interval (CI), 0.53 to 1.00], with 75% sensitivity and 100% specificity for ctDNA analysis compared to tumor DNA. The single patient with an *ESR1* mutation detected in tumor, but not in plasma, had a *PIK3CA* mutation in tumor that was also not detectable in plasma by digital PCR, suggesting that discordance reflected very low levels of ctDNA release. To assess technical reproducibility and the potential to mail samples in cell-free DNA preservative tubes, we separately collected blood samples into EDTA tubes and into DNA preservative Streck tubes. EDTA tubes were processed within 2 hours, whereas preservative tubes were mailed and processed 48 to 72 hours after venesection. There was 100% agreement between repeat plasma samples processed entirely separately, taken from the same patient at the same

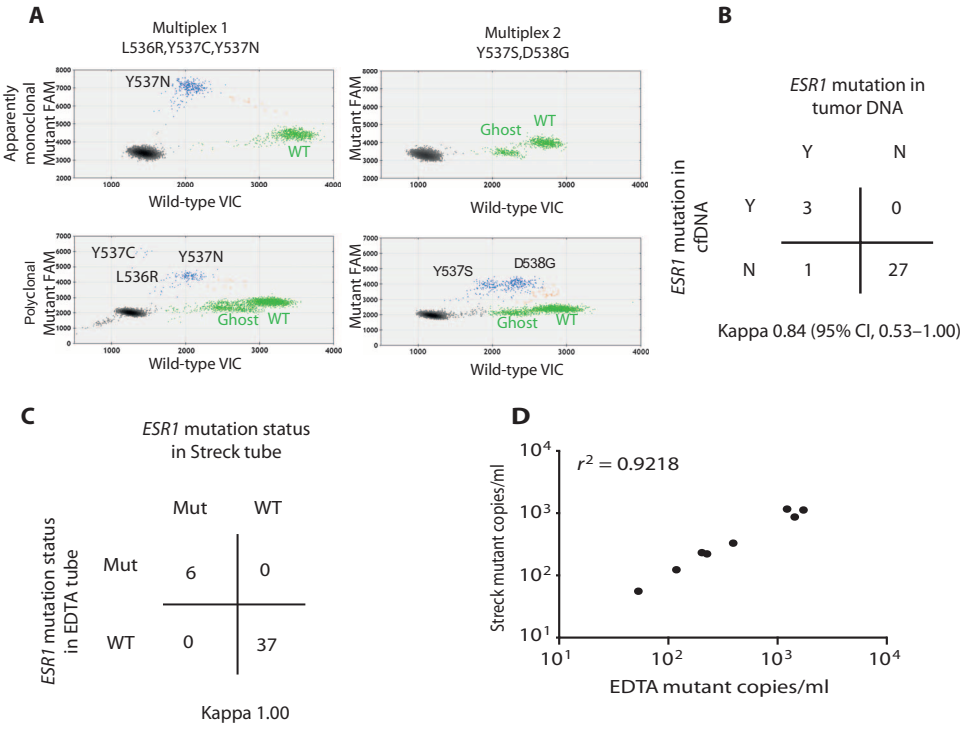

Fig. 1. Assessment of *ESR1* in ctDNA with multiplex digital PCR assays has analytical and clinical validity. (**A**) High-sensitivity multiplex digital PCR for LBD *ESR1* mutations. Representative digital PCR analysis of plasma DNA from two separate patients. Top: Detection of an apparently monoclonal Y537N (*c.1609T>A*) mutation. Bottom: Detection of polyclonal *ESR1* mutations. The presence of all five mutations was confirmed by uniplex assays, with Y537C (*c.1610A>G*) and L536R (*c.1607T>G*) detectable in low amounts. In each plot, green dots represent VIC-labeled wild type (WT) DNA (except for the population labeled as "Ghost," which represents droplets with mutations different from those analyzed in the assay), blue dots represent FAM-labeled mutant DNA, brown dots represent droplets containing both WT and mutant DNA, and black dots are droplets with no DNA incorporated. (**B**) Comparison of *ESR1* mutation calling between contemporaneous tumor biopsies and ctDNA plasma samples from 31 patients with advanced breast cancer, with overall 97% agreement between tumor DNA and ctDNA analysis ($\kappa = 0.84$; 95% CI, 0.53 to 1.0). Detection of *ESR1* in ctDNA has 100% positive predictive value for tumor *ESR1* mutation status and 96.4% negative predictive value. (**C**) Comparison of *ESR1* mutation calling between repeat samples from the same 43 patients. Two different tubes (one EDTA tube and one cell-free DNA Streck tube) were used at the same blood draw and processed entirely separately. There was 100% agreement between assays ($\kappa = 1.0$; 95% CI, not estimable), with exact concordance of the mutation called between samples. (**D**) Correlation between mutation abundance (mutant copies per milliliter of plasma) assessed in EDTA and Streck tubes in *ESR1* mutant plasma samples. $r^2 = 0.92$, Pearson's correlation coefficient.

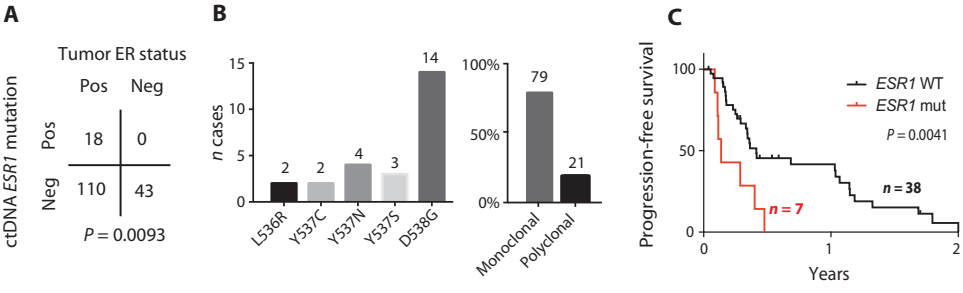

Fig. 2. Detection of *ESR1* mutations in plasma predicts lack of sensitivity to subsequent AI therapy. (**A**) *ESR1* ctDNA analysis by multiplex digital PCR in 171 patients with advanced breast cancer. *ESR1* mutations are detected exclusively in plasma of patients with ER-positive advanced breast cancer ($P = 0.0093$, χ^2 test). (**B**) Left: Profile of *ESR1* mutations detected in ctDNA. Right: Percentage of cases with apparently monoclonal (79%) or polyclonal (21%) *ESR1* mutations. (**C**) PFS on AI therapy after ctDNA analysis for patients with *ESR1* mutant and WT ctDNA (HR, 3.1; 95% CI, 1.9 to 23.1; $P = 0.0041$, log-rank test).

blood draw (Fig. 1C; κ = 1.00; 95% CI, not estimable), with a high correlation of *ESR1* mutation abundance (Fig. 1D), providing evidence of both extremely high technical reproducibility and the ability to mail unprocessed samples in preservative tubes. In a dilution experiment, we showed that the digital PCR assays are able to detect as few as three copies of the mutant allele in an excess of wild-type DNA (fig. S1A).

ESR1 mutations were detected in the plasma of 10.5% (18 of 171; 95% CI, 6 to 16) of patients with advanced breast cancer, exclusively in patients with ER-positive breast cancer (ER-positive 14% versus ER-negative 0%; $P = 0.0093$, χ^2 test; Fig. 2A). All patients with *ESR1* mutations detected had previous AI exposure, with a median duration of previous exposure of 23 months (range, 5.9 to 141.4) (Table 1). None (0 of 22; 95% CI, 0 to 15) of the patients with previous tamoxifen without AI exposure had detectable *ESR1* mutations. *ESR1* mutation ctDNA abundance was highly correlated between multiplex and uniplex mutation assays (fig. S1B), with a distribution of mutations that was highly similar to previously published data (Fig. 2B) (*8*–*11*). *ESR1* mutations were shown to be overtly polyclonal in 21% of *ESR1* mutant patients and apparently monoclonal in the remaining 79% of patients (Fig. 2B).

Detection of *ESR1* mutations predicts for relative resistance to subsequent AI-based therapy

We investigated sensitivity to hormonal therapy after ctDNA assessment. Patients with *ESR1* mutation(s) detected in plasma had a substantially shorter progression-free survival (PFS) on subsequent AI-based therapy, whether given as therapy after disease progression [fig. S2; hazard ratio (HR), 3.7; 95% CI, 1.9 to 76.9; $P = 0.008$, log-rank test] or including the duration of AI given as maintenance therapy after response to previous chemotherapy (Fig. 2C; HR, 3.1; 95% CI, 1.9 to 23.1; $P = 0.0041$, log-rank test). There were not enough patients who had exposure to the ER degrader fulvestrant after ctDNA assessment to assess the activity of fulvestrant in this population.

ESR1 mutations are predominantly acquired during the treatment of metastatic disease

To investigate the factors that associated with detection of *ESR1* mutations in ctDNA, we looked for differences in clinical and pathological factors between ER-positive cancers that were *ESR1* wild type and mutant in ctDNA (Table 1). There was no difference in grade, *HER2* status, previous chemotherapy exposure, cumulative duration of previous AI therapy, or sites of metastasis. Although all patients with detectable *ESR1* mutation had previous AI exposure, patients with detectable *ESR1* mutations had less frequent AI exposure in the adjuvant setting (*ESR1* mutant 16% versus *ESR1* wild type 45%, $P = 0.0216$) and more frequent AI exposure in the metastatic setting (*ESR1* mutant 95% versus *ESR1* wild type 36%, $P < 0.0001$, Table 1). Within the subset of patients who had AI exposure only in the metastatic setting, there was no difference in cumulative duration of previous AI exposure (23.3 months *ESR1* wild type versus 23.0 months *ESR1* mutant; $P = 0.82$, Mann-Whitney *U* test), number of courses of previous endocrine therapy (median, 2.0 versus 1.5; $P = 0.39$), or duration of first AI exposure (13.2 versus 18.1 months, respectively; $P = 0.47$).

We further investigated whether the timing of previous AI exposure influenced the prevalence of *ESR1* mutations. Strikingly, patients who had received previous AI in the adjuvant setting for the treatment of micrometastatic disease, whether followed by further therapy in the metastatic setting, had a substantially lower prevalence of *ESR1* mutation(s) compared to patients who first received previous AI only for the treatment of metastatic breast cancer (5.8% versus 36.4%; Fig. 3A; $P = 0.0002$, χ^2 test). The subset of patients who had ctDNA samples taken at the time of recurrence on adjuvant AI also had a low rate of *ESR1* mutation in ctDNA (4.8% 1 of 21), suggesting that the difference did not reflect loss of *ESR1* mutation due to time between exposure to

Table 1. Characteristics of patients with advanced ER-positive breast cancer grouped by *ESR1* status.

	ESR1 wild type	*ESR1* mutant	*P*
n	109	19	
Median age (years)	58	64	0.9*
Grade			
1	8	1	0.89†
2	59	10	
3	38	5	
HER2-positive	17%	11%	0.61†
Disease presentation‡			
Relapsed	90	15	0.74†
De novo	19	4	
Visceral disease	60%	79%	0.07†
Bone disease	65%	84%	0.12†
Previous chemotherapy			
Adjuvant	50%	42%	0.62†
Courses metastatic chemotherapy			
0	68	9	0.63†
1	22	5	
2	13	3	
3+	6	2	
Previous endocrine therapy			
Adjuvant			
Tamoxifen ± ovarian suppression	56%	53%	0.8†
Aromatase inhibitor	45% (49/109)	16% (3/19)	0.017†
Advanced			
Tamoxifen ± ovarian suppression	19% (20/109)	48% (9/19)	0.0053†
Aromatase inhibitor	46% (50/109)	95% (18/19)	<0.0001†
First exposure to AI			
Adjuvant	49	3	0.0002†
Advanced	28	16	
No AI exposure	32	0	
Median cumulative duration of previous AI exposure	31.8 months	23.4 months	0.42*

*Unpaired *t* test. †χ^2 test. ‡Presentation of advanced disease is defined as de novo (advanced at first presentation) or relapsed (relapsed after previous presentation with early-stage cancer).

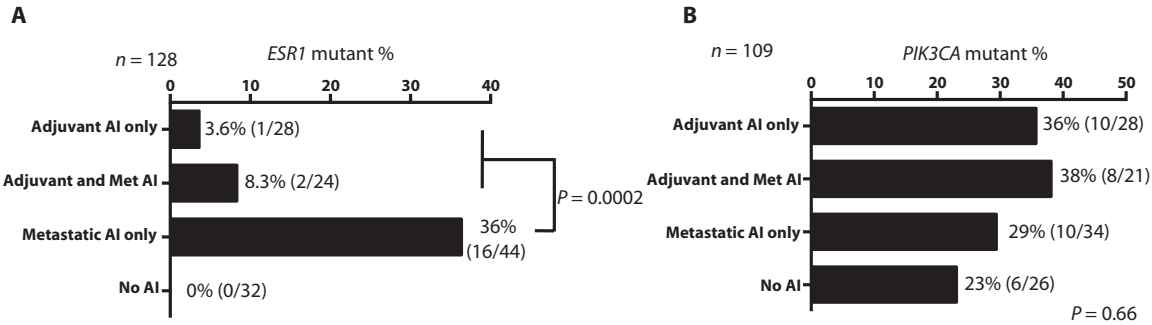

Fig. 3. *ESR1* mutations are rarely acquired during adjuvant AI and frequently during metastatic AI therapy. (**A**) *ESR1* ctDNA mutation rate split by timing of patients' exposure to AI therapy or no previous exposure to AI therapy. $P < 0.0001$, χ^2 test overall; $P = 0.0002$, χ^2 test comparing metastatic AI only to previous exposure first in the adjuvant setting. (**B**) *PIK3CA* ctDNA mutation rate, assessed with multiplex digital PCR assay, split by timing of patients' exposure to AI therapy, or no previous exposure to AI therapy. Samples from 19 patients included in (A) were not analyzed because plasma was exhausted. $P = 0.66$, χ^2 test.

AI and taking of plasma sample for ctDNA analysis. A further confounding factor could be that plasma samples contained no ctDNA in patients exposed to AI in the adjuvant setting. To address this, we assessed the prevalence of hotspot *PIK3CA* mutations in plasma DNA and found similar rates of *PIK3CA* mutation across all groups (Fig. 3B), suggesting that differences in ctDNA abundance did not explain the observation.

We assessed the rate of *ESR1* mutations only in patients with known detectable ctDNA by assessing the rate of *ESR1* mutation only in samples with another mutation detected in plasma DNA. To extend the power of this analysis beyond *PIK3CA* mutations identified with digital PCR, we sequenced plasma samples from 76 patients with massive parallel sequencing (MPS) using a custom Ion Torrent amplicon sequencing panel (table S3), calling mutations with an allele frequency of >3%. Mutations with an allele frequency of 3 to 10% were additionally confirmed by digital PCR. We sequenced plasma from seven patients with *ESR1* mutations identified by digital PCR and found the corresponding mutation in four (57%) of these patients, reflecting the higher sensitivity of digital PCR for low allele frequencies. Of the 69 patients without an *ESR1* LBD mutation by digital PCR, none had an *ESR1* LBD mutation by MPS ($P < 0.0001$, χ^2 test). Using MPS, we identified an additional mutation (other than *PIK3CA*) in 13 patients. We next assessed the rate of *ESR1* mutations only in the 49 patients who had experimental evidence of ctDNA being present, by either *PIK3CA* digital PCR or plasma DNA MPS. *ESR1* mutations were found in 7% (1 of 15) of patients exposed to AI in the adjuvant setting only, in 14% (2 of 14) of patients with exposure in both adjuvant and metastatic settings, and in 42% (5 of 12) of patients with AI exposure only in the metastatic setting (Fig. 4A). Our data suggest that *ESR1* mutations were present at a higher rate in patients exposed to AI in the metastatic setting and only rarely occur in patients exposed to AI in the adjuvant setting.

To confirm these observations, we examined three independent cohorts. The first independent cohort was from 49 patients with tumor biopsies taken at the time of recurrence or at progression on AI. We identified no mutations in patients exposed to AI in the adjuvant setting (0 of 32; 95% CI, 0 to 10.9; Fig. 4B), confirming the low incidence of *ESR1* mutations in patients treated in the adjuvant setting. Conversely, mutations were identified in 12% (2 of 17) of patients exposed to AI in the metastatic setting. For the second cohort, we collected plasma samples from an additional independent set of 28 patients with metastatic breast cancer, 18 of whom had previous AI treatment. In those with previous AI therapy in the adjuvant setting, we identified *ESR1* mutations in 0% (0 of 7) of patients, whereas in those who had received previous AI only in the metastatic setting, we identified *ESR1* mutations in 36% (4 of 11) of patients. For the third independent cohort, we re-examined the timing of AI exposure on the previously published index series of *ESR1* mutant cancers, none of which had previous exposure to AI in the adjuvant setting alone (Fig. 4C) (*9*).

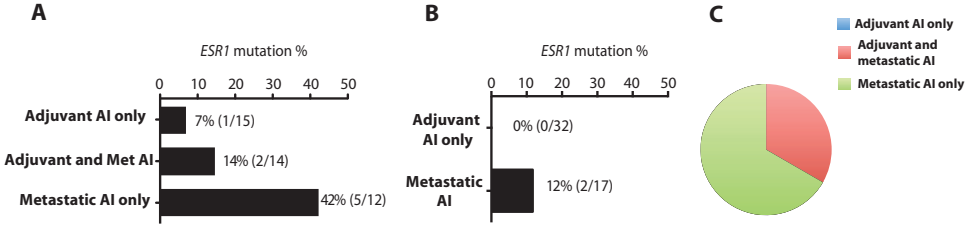

Fig. 4. Validation and independent series confirm the importance of timing of previous AI exposure for *ESR1* mutation selection. (**A**) *ESR1* mutation rate assessed only in patients with detection of a mutation other than *ESR1* in plasma DNA. $P = 0.061$, χ^2 test overall; $P = 0.035$, adjuvant AI only versus metastatic AI only. (**B**) Assessment of *ESR1* mutation rate in an independent series of 49 breast tumor biopsies that had recurred after previous AI therapy. No *ESR1* mutations were identified in breast tumor biopsies relapsing after adjuvant AI (0%; 95% CI, 0 to 10.9). (**C**) Reassessment of a second independent series of *ESR1* mutant–positive cancers, with timing of previous AI therapy (*9*).

ESR1 mutations can be selected to become the dominant clone in the cancer

We assessed the relative clonality of *ESR1* mutations in ctDNA, comparing the abundance of *ESR1* mutation to other common driver mutations identified with *PIK3CA* digital PCR and ctDNA MPS. In a patient with sequential samples taken during metastatic treatment, an *ESR1* mutation was shown to be selected by previous AI treatment for metastatic cancer to become the dominant clone (Fig. 5A). We assessed the relative clonal dominance of *ESR1* mutation, comparing the allele frequency of the *ESR1* mutation with allele frequency of *PIK3CA* on the same plasma sample. We assumed that most of the *PIK3CA* mutations are clonal in ER-positive breast cancers and therefore that the relative allele

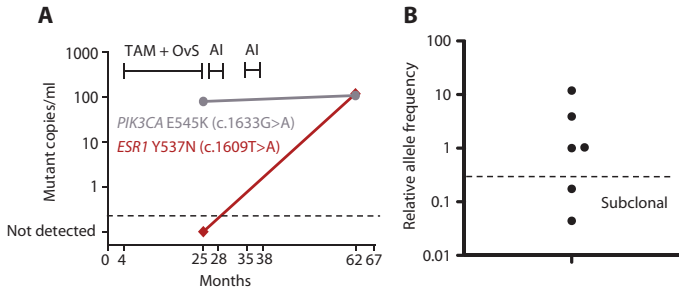

Fig. 5. *ESR1* mutations may be selected to become the dominant clone in the cancer. (**A**) Serial ctDNA analysis in a patient with plasma samples taken before and after exposure to AI for metastatic breast cancer. Tumor *PIK3CA* mutation is detected in both plasma samples, whereas *ESR1* mutation is only detected after developing resistance to AI. OvS, ovarian suppression (goserelin, followed by bilateral salpingo-oophorectomy); TAM, tamoxifen. (**B**) Relative abundance of *ESR1* mutations in ctDNA compared to abundance of other tumor-derived mutations detected in ctDNA. Below dotted line (0.25) suggests likely subclonal mutations.

frequency would give an assessment of clonal dominance (within wide limits to take account of potential copy number variation in the tumor). We included an additional patient with a *PTEN* mutation identified by MPS. This analysis suggested that the *ESR1* mutation may be clonally dominant in the tumors of four patients, whereas the *ESR1* mutation was likely subclonal in the tumors of two patients (Fig. 5B). These data suggest that assessment of *ESR1* mutation clonality is likely to be important in the development of therapeutics targeting the mutant ER. Finally, we investigated for evidence of loss of *ESR1* mutation with time after AI exposure (*15*). The rate of detection of *ESR1* mutation was unaltered between patients with samples taken at the time of completing AI therapy for metastatic cancer or >6 months later [samples <6 months from completing AI therapy 22% (11 of 50) versus >6 months 41% (7 of 17) *ESR1* mutant; $P = 0.12$, χ^2 test], suggesting that once selected by previous AI therapy, the *ESR1* mutation may persist in the tumor through subsequent therapy.

DISCUSSION

ctDNA analysis has the potential to allow noninvasive analysis of tumor genetic alterations in advanced cancer. Here, we demonstrate that ctDNA analysis has analytical and clinical validity in the identification of hotspot LBD *ESR1* mutations in the plasma of advanced breast cancer patients and has possible clinical utility in identifying a group of patients who derive very limited benefit from further AI therapy.

Our data provide evidence that the mechanism of resistance to targeted therapy, specifically AIs, may differ substantially depending on the setting of exposure. *ESR1* mutations are selected frequently during treatment for metastatic breast cancer, likely through selection of rare *ESR1* mutant subclones that were present in low amounts before therapy as a result of genetic intratumoral heterogeneity and clonal diversity in the cancer (fig. S3). However, our data suggest that in patients treated in the adjuvant setting with micrometastatic disease, *ESR1* mutations are selected/acquired less frequently, potentially due to a lack of genetic diversity in micrometastatic disease. We speculate that the tumor bulk of micrometastatic disease may be sufficiently low that rare *ESR1* mutant subclones are not present and cannot therefore be selected by therapy (fig. S3). We were unable to provide direct evidence that *ESR1* mutations preexist before therapy in the metastatic setting. However, we do show that *ESR1* mutations are frequently monoclonal, are therefore likely derived from a single cell, arise over a median of 23 months' exposure, and frequently become the dominant clone in the cancer. Given the doubling rate of ER-positive breast cancer (*16*), it is relatively unlikely that a single cell could repopulate the metastatic cancer in this time, and therefore, our data suggest that *ESR1* mutations likely preexist in the tumor before exposure. However, it is also possible that in cancers with a longer duration of previous AI exposure, the mutation could be acquired during therapy, initiated through mutagenic processes such as the APOBEC enzymes (*17*).

Our data illustrate the potential value of ctDNA analysis and the ability to access large unbiased cohorts of patients with pretreated advanced cancer without the potential selection biases inherent in tissue biopsy cohorts, where patients are selected on the basis of suitability for biopsy. Nevertheless, our study has a number of limitations. The studied population is heterogeneously treated, and the sample size does not allow us to examine whether *ESR1* mutation detection predicts sensitivity to specific hormone therapies or combinations, for example, fulvestrant or everolimus plus exemestane, respectively. We could not assess the lead time between emergence of *ESR1* mutations in ctDNA and clinical progression of the disease because of limited longitudinal sampling. Here, we did not examine less frequent *ESR1* mutations (for example, E380Q or S463P), partly because their function has not been studied extensively yet. In line with previous publications, we found D538G to be the most common mutation identified in plasma DNA, although we had insufficient data to address whether there were clinical differences between different *ESR1* mutations in the LBD. Finally, in lung cancer, T790M *EGFR* mutations selected by previous *EGFR* targeted therapy can be lost during subsequent treatment, possibly because the T790M clone may proliferate more slowly and be "overtaken" by residual wild-type *EGFR* clones once the selective pressure of *EGFR* targeted therapy is removed. A similar result has been reported for selected *KRAS* mutations in colorectal cancer treated with EGFR inhibitors (*15*). This could provide an explanation for the low rates of *ESR1* mutations in the adjuvant AI setting, if there was intervening non-AI treatment before sampling. We provide two controls to suggest that this is not the main explanation: the subset of patients with a ctDNA sample taken at the time of relapse on AI had very low *ESR1* mutation detection, and we observed no mutations in the independent series of tumor biopsies taken at relapse on AI therapy. In addition, our data suggest that *ESR1* mutations remain readily detectable in ctDNA many months and years after stopping AI therapy, suggesting possible differences between selected *ESR1* mutations in breast cancer and *KRAS* in colorectal cancer.

Our data provide evidence for the clinical validity of ctDNA *ESR1* mutation testing and support ctDNA screening to select patients for prospective clinical trials with drugs that target *ESR1* mutations, such as oral ER degraders, which are in early clinical development. *ESR1* mutations are rarely acquired during adjuvant AI therapy but are commonly selected by therapy for metastatic disease, providing evidence that the mechanisms of resistance to targeted therapy may be substantially different between the treatment of micrometastatic and overt metastatic cancer.

MATERIALS AND METHODS

Study design

We collected a series of plasma DNA samples from patients with advanced breast cancer to assess the potential utility of *ESR1* mutation analysis in

ctDNA. We developed multiplex digital PCR assays for hotspot LBD mutations and used these assays to screen for *ESR1* mutations. In parallel, a subset of patients had biopsy samples obtained contemporaneously with plasma samples to assess agreement with tumor biopsy, and repeat plasma sampling to assess reproducibility and the ability to mail samples in preservative tubes. We investigated the relationship between detection of *ESR1* mutation and sensitivity to subsequent hormonal therapy. We also identified the clinical and pathological features that associated with the presence of an *ESR1* mutation and validated these associations in an independent series of 49 tumor biopsies taken on progression on AI therapy.

Patients

We analyzed 171 consecutive patients with advanced breast cancer at the Royal Marsden Hospital (RMH), who consented to tissue collection studies approved by multicenter research ethics committees (ref. nos. 10/H0805/50 and 11/LO1595). All patients had recently relapsed or progressed after previous therapy.

ER, progesterone receptor (PgR), and human epidermal growth factor receptor 2 (HER2) were assessed in a single laboratory at the Royal Marsden Histopathology department (or reviewed by the RMH when reported from a referring hospital) using standard criteria.

For patients who had biopsy of recurrent cancer, this biopsy was used to define the receptor status, and for the remaining patients, the pathology of the primary cancer was used. For patients who had biopsies from multiple metachronous metastatic sites, the most recent biopsy was used to define the receptor status. Patients who presented with primary breast cancer simultaneously with metastatic disease were recorded as having biopsy of recurrent cancer. Table 1 illustrates the main clinicopathological characteristics of ER-positive patients in this cohort, and table S1 shows the whole cohort.

Patients with previous AI exposure were divided by time of first exposure to AI in the adjuvant setting (treatment with either preoperative AI or adjuvant AI after surgery for early breast cancer or isolated local recurrence and before metastatic relapse) or the metastatic setting (first treatment with an AI after metastatic relapse). Patients were considered to have had plasma samples taken "at time of relapse on AI therapy" when blood was taken within 6 months of stopping adjuvant AI. To analyze associations with subsequent AI-based therapy, PFS was defined as the time from starting AI to documented disease progression or death. Patients receiving AI and an anti-HER2 agent concomitantly were excluded from this analysis. For patients who received chemotherapy after the blood test and then went onto maintenance AI therapy, the baseline date for PFS analysis was the starting date of AI.

An independent validation cohort consisted of a separate series of 49 patients with recurrent breast cancer who were all pretreated with an AI before the recurrent disease biopsy (*18*). For 43 of 49 of these cases, a biopsy sample obtained before AI therapy was also available for assessment. First exposure to AI was in the adjuvant setting for 32 of these patients and in the metastatic setting for 17 patients using the above definitions. A further, entirely independent, set of plasma samples was also collected from an additional 28 patients with metastatic breast cancer for additional independent validation.

Processing and DNA extraction from tumor tissue

Thirty-one patients in our cohort had tumor biopsies contemporaneous with the plasma samples. Archival formalin-fixed and paraffin-embedded (FFPE) tissue blocks were retrieved, and sections (4 to 8 × 4 μm) were cut from these blocks, stained with Nuclear Fast Red, and microdissected to achieve >70% tumor cell purity using a hematoxylin and eosin–stained slide to guide manual microdissection. Tumor DNA was isolated using the QIAamp DNA FFPE Tissue Kit (Qiagen) as per the manufacturer's instructions. DNA was eluted in 50 to 100 μl of ATE buffer, depending on the amount of tumor on the slides, and stored at −20°C until quantification. For the validation cohort, tumor DNA was isolated using the Qiagen AllPrep DNA/RNA FFPE Kit as per the manufacturer's instructions.

Processing of plasma and extraction of circulating DNA

Blood collected in Vacutainer EDTA Blood Collection Tubes (BCT) was processed within 2 hours of sample collection and centrifuged at 1600*g* for 20 min to separate the plasma from the peripheral blood cells. Plasma was stored at −80°C until DNA extraction. DNA was extracted from 2 ml of aliquots of plasma using the QIAamp Circulating Nucleic Acid Kit (Qiagen) according to the manufacturer's instructions. The DNA was eluted into 50 μl of buffer AVE and stored at −20°C until quantification. For a subset of patients, to test concordance and alternative methods of blood processing, blood was also placed in Streck Cell-Free DNA BCT tubes at the same visit as the EDTA sample, and shipped at room temperature, with plasma separated 48 to 72 hours after venesection.

DNA quantifications from tissue and/or plasma

DNA isolated from tissue or plasma was quantified on a Bio-Rad QX200 Droplet Digital PCR (ddPCR) System using ribonuclease (RNase) P as the reference gene. One microliter of eluate was added to a ddPCR containing 10 μl of ddPCR Supermix for probes (Bio-Rad) and 1 μl of TaqMan Copy Number Reference Assay, human, RNase P (Life Technologies) in a total volume of 20 μl. The reaction was partitioned into ~14,000 droplets per sample in a QX200 droplet generator according to the manufacturer's instructions. Emulsified PCRs were run on a 96-well plate on a G-Storm GS4 thermal cycler, incubating the plates at 95°C for 10 min followed by 40 cycles at 95°C for 15 s and 60°C for 60 s, then 10-min incubation at 98°C. The temperature ramp increment was 2.5°C/s for all steps. Plates were read on a Bio-Rad QX200 droplet reader with QuantaSoft v1.6.6.0320 software from Bio-Rad. At least two negative control wells with no DNA were included in every run. The amount of amplifiable RNase P DNA was calculated from the concentration provided by the software.

Development of LBD ESR1 mutation digital PCR assays

We designed primer probe combinations for each of the most common *ESR1* mutations (p.L536R, p.Y537S, p.Y537N, p.Y537C, and p.D538G) (table S2) using Primer3Plus or Life Technologies' custom SNP genotyping assay tool. Primers and probes were analyzed for the presence of hairpins, secondary structures, or heterodimer/homodimer formation. Primers were analyzed for specificity of the primer pair to their amplicon using University of California, Santa Cruz, ePCR tool (http://genome.ucsc.edu/cgi-bin/hgPcr?command=start). Digital PCR conditions were optimized with a temperature gradient to identify the optimal annealing/extension temperature using wild-type DNA spiked with a mutant synthetic oligonucleotide (table S2) on a QX200 ddPCR system (Bio-Rad) using TaqMan chemistry. We developed multiplex assays varying the concentration of the fluorescent probes to differentiate mutations on the basis of fluorescence intensity (*19*). We selected the two optimal

multiplex assay combinations (multiplexes 1 and 2) and probe concentrations as shown in table S2.

Limit of detection of ESR1 assays

Genomic DNA (gDNA) was extracted from the *ESR1* wild-type human mammary gland cell line CAMA-1 (American Type Culture Collection HTB-21) with DNeasy Blood and Tissue Kit (Qiagen) as per the manufacturer's instructions. DNA was quantified using Quant-iT PicoGreen dsDNA Assay Kit (Life Technologies) as per the manufacturer's instructions. We spiked 15,000 genomes of STR-typed CAMA-1 gDNA with 200, 100, 5, and 3 copies of mutant D538G DNA and ran a uniplex digital PCR with the primers and probes for this mutation (table S2) as described above. We calculated the number of copies assayed versus the frequency of mutation detected after digital PCR cycling and plotted it to assess the lower limit of detection for this assay.

Hotspot PIK3CA mutation digital PCR assays

Digital PCR assays for the four most common occurring mutations in the *PIK3CA* gene—E542K (*c.1624G>A*), E545K (*c.1633G>A*), H1047L (*c.3140A>T*), and H1047R (*c.3140A>G*)—were developed as for *ESR1 LBD* assays, using TaqMan probes [FAM (fluorescein)–labeled for mutant and VIC-labeled for wild type], and have been described previously (*20*). We developed a multiplex assay varying the concentration of the fluorescent probes to differentiate mutations on the basis of fluorescence intensity as above, and we selected the optimal multiplex assay combination and probe concentrations, which enabled us to test for the four hotspot mutations in one single reaction. *PIK3CA* mutation testing in ctDNA was performed in a subgroup of the cohort (109 of 128 ER-positive patients) who had sufficient residual plasma for analysis.

Digital PCR analysis of circulating free DNA and tumor tissue DNA

Digital PCR was performed on a QX200 digital PCR system (Bio-Rad) using the assays described in table S2. For plasma samples, circulating free DNA (cfDNA) equivalent to 250 μl of plasma was used per multiplex assay. For tumor tissue DNA, 1 ng was used per multiplex assay. PCRs were prepared with digital PCR Supermix for probes (Bio-Rad) and partitioned into a median of ~14,000 droplets per well in a QX200 droplet generator according to the manufacturer's instructions. Emulsified PCRs were run on a 96-well plate on a G-Storm GS4 thermal cycler, incubating the plates at 95°C for 10 min followed by 40 cycles of 95°C for 15 s and 60°C for 60 s, then 10-min incubation at 98°C. The temperature ramp increment was 2.5°C/s for all steps. Plates were read on a Bio-Rad QX200 droplet reader with QuantaSoft v1. 6.6.0320 software from Bio-Rad to assess the number of droplets positive for mutant DNA, wild-type DNA, both, or neither. At least two negative control wells with no DNA were included in every run. A mutation was considered positive with at least two *ESR1* mutant (or *PIK3CA*) droplets. The multiplex digital PCR was performed for mutation detection, and the individual mutation or mutations present were subsequently confirmed with uniplex digital PCR assays.

Digital PCR analysis

The concentration of mutant DNA (copies of mutant DNA per droplet) was estimated from the Poisson distribution. The number of mutant copies per droplet was calculated as Mmu = –ln (1 – (nmu/n)), where nmu is the number of droplets positive for mutant-FAM probe and n is the total number of droplets. The DNA concentration in the reaction was estimated as follows: MDNAconc = –ln (1 – (nDNAconc/n)), where nDNAconc is the number of droplets positive for mutant-FAM probe and wild type–VIC probe and n is the total number of droplets. The mutation allele fraction = Mmu/MDNAconc. The number of mutant copies per milliliter of plasma was estimated from the mutation allele fraction by taking into account the number of wells run for the sample and the volume equivalent of plasma run, and the mean volume of a droplet (0.89 pl) using the following formula:

Mutant copies per ml = (total number of droplets positive for FAM and/or VIC × 20,000)/total number of droplets read/0.89 × (number of droplets/volume of plasma equivalents)

Ion Torrent Proton sequencing of plasma samples

Sequencing libraries were prepared with a custom Ion AmpliSeq Breast Cancer Panel targeting 14 known breast cancer driver and focal mutations (table S3) using the Ion AmpliSeq Library Preparation protocol with 3 ng of cfDNA, according to the manufacturer's instructions. After barcoding, libraries were quantified using qPCR, diluted to 100 pM, and pooled. Libraries were templated with the Ion OneTouch2 system (Life Technologies) and sequenced on a PI chip using the Ion PI OT2 200 Kit (Life Technologies), 520 flows, and an average amplicon length of 97 bases to a mean depth of ×9183. The sequencing resulted in 1,042,543 to 5,763,164 reads per sample.

Ion Torrent Variant Caller v4.0-r73742 with no hotspot region and configuration "Germ Line Low Stringency" was used for calling variants. Read counts for all positions were computed using pileup [SAMtools v1.1 (*21*)], and these data were analyzed for possible variants using custom perl and R scripts. Variants at >3% reported by both analysis methods and not reported in 1000 Genomes Project database (www.1000genomes.org) were identified as possible somatic mutations. The data were cross-referenced against the Cosmic database v70 (cancer.sanger.ac.uk) to identify possible hotspot mutations. Variants not appearing in the 1000 Genomes database were taken forward for validation by digital PCR assays.

Statistical analysis

All statistical analysis was performed with GraphPad Prism version 6.0 or Microsoft Excel. Unless stated otherwise, P values were two-tailed and considered significant if $P < 0.05$.

SUPPLEMENTARY MATERIALS

www.sciencetranslationalmedicine.org/cgi/content/full/7/313/313ra182/DC1
Fig. S1. *ESR1* LBD digital PCR assays are sensitive and highly reproducible.
Fig. S2. Patients with *ESR1* mutation have poor outcome on subsequent AI therapy.
Fig. S3. A theoretical model explains the evolution of *ESR1* mutations during treatment for metastatic breast cancer.
Table S1. Clinical and pathological characteristics of the series of patients with advanced cancer.
Table S2. *ESR1* mutations analyzed and experimental conditions (provided as an Excel file).
Table S3. Ion AmpliSeq Breast Cancer driver and focal mutation gene panel.

REFERENCES AND NOTES

1. N. C. Turner, J. S. Reis-Filho, Genetic heterogeneity and cancer drug resistance. *Lancet Oncol.* **13**, e178–e185 (2012).
2. A. B. Turke, K. Zejnullahu, Y.-L. Wu, Y. Song, D. Dias-Santagata, E. Lifshits, L. Toschi, A. Rogers, T. Mok, L. Sequist, N. I. Lindeman, C. Murphy, S. Akhavanfard, B. Y. Yeap, Y. Xiao, M. Capelletti,

A. J. Iafrate, C. Lee, J. G. Christensen, J. A. Engelman, P. A. Jänne, Preexistence and clonal selection of *MET* amplification in *EGFR* mutant NSCLC. *Cancer Cell* **17**, 77–88 (2010).
3. P. J. Campbell, S. Yachida, L. J. Mudie, P. J. Stephens, E. D. Pleasance, L. A. Stebbings, L. A. Morsberger, C. Latimer, S. McLaren, M.-L. Lin, D. J. McBride, I. Varela, S. A. Nik-Zainal, C. Leroy, M. Jia, A. Menzies, A. P. Butler, J. W. Teague, C. A. Griffin, J. Burton, H. Swerdlow, M. A. Quail, M. R. Stratton, C. Iacobuzio-Donahue, P. A. Futreal, The patterns and dynamics of genomic instability in metastatic pancreatic cancer. *Nature* **467**, 1109–1113 (2010).
4. N. Houssami, P. Macaskill, R. L. Balleine, M. Bilous, M. D. Pegram, HER2 discordance between primary breast cancer and its paired metastasis: Tumor biology or test artefact? Insights through meta-analysis. *Breast Cancer Res. Treat.* **129**, 659–674 (2011).
5. L. Ding, M. J. Ellis, S. Li, D. E. Larson, K. Chen, J. W. Wallis, C. C. Harris, M. D. McLellan, R. S. Fulton, L. L. Fulton, R. M. Abbott, J. Hoog, D. J. Dooling, D. C. Koboldt, H. Schmidt, J. Kalicki, Q. Zhang, L. Chen, L. Lin, M. C. Wendl, J. F. McMichael, V. J. Magrini, L. Cook, S. D. McGrath, T. L. Vickery, E. Appelbaum, K. DeSchryver, S. Davies, T. Guintoli, L. Lin, R. Crowder, Y. Tao, J. E. Snider, S. M. Smith, A. F. Dukes, G. E. Sanderson, C. S. Pohl, K. D. Delehaunty, C. C. Fronick, K. A. Pape, J. S. Reed, J. S. Robinson, J. S. Hodges, W. Schierding, N. D. Dees, D. Shen, D. P. Locke, M. E. Wiechert, J. M. Eldred, J. B. Peck, B. J. Oberkfell, J. T. Lolofie, F. Du, A. E. Hawkins, M. D. O'Laughlin, K. E. Bernard, M. Cunningham, G. Elliott, M. D. Mason, D. M. Thompson Jr., J. L. Ivanovich, P. J. Goodfellow, C. M. Perou, G. M. Weinstock, R. Aft, M. Watson, T. J. Ley, R. K. Wilson, E. R. Mardis, Genome remodelling in a basal-like breast cancer metastasis and xenograft. *Nature* **464**, 999–1005 (2010).
6. L. A. Diaz Jr., R. T. Williams, J. Wu, I. Kinde, J. R. Hecht, J. Berlin, B. Allen, I. Bozic, J. G. Reiter, M. A. Nowak, K. W. Kinzler, K. S. Oliner, B. Vogelstein, The molecular evolution of acquired resistance to targeted EGFR blockade in colorectal cancers. *Nature* **486**, 537–540 (2012).
7. S. Misale, R. Yaeger, S. Hobor, E. Scala, M. Janakiraman, D. Liska, E. Valtorta, R. Schiavo, M. Buscarino, G. Siravegna, K. Bencardino, A. Cercek, C.-T. Chen, S. Veronese, C. Zanon, A. Sartore-Bianchi, M. Gambacorta, M. Gallicchio, E. Vakiani, V. Boscaro, E. Medico, M. Weiser, S. Siena, F. Di Nicolantonio, D. Solit, A. Bardelli, Emergence of *KRAS* mutations and acquired resistance to anti-EGFR therapy in colorectal cancer. *Nature* **486**, 532–536 (2012).
8. K. Merenbakh-Lamin, N. Ben-Baruch, A. Yeheskel, A. Dvir, L. Soussan-Gutman, R. Jeselsohn, R. Yelensky, M. Brown, V. A. Miller, D. Sarid, S. Rizel, B. Klein, T. Rubinek, I. Wolf, D538G mutation in estrogen receptor-α: A novel mechanism for acquired endocrine resistance in breast cancer. *Cancer Res.* **73**, 6856–6864 (2013).
9. W. Toy, Y. Shen, H. Won, B. Green, R. A. Sakr, M. Will, Z. Li, K. Gala, S. Fanning, T. A. King, C. Hudis, D. Chen, T. Taran, G. Hortobagyi, G. Greene, M. Berger, J. Baselga, S. Chandarlapaty, *ESR1* ligand-binding domain mutations in hormone-resistant breast cancer. *Nat. Genet.* **45**, 1439–1445 (2013).
10. D. R. Robinson, Y.-M. Wu, P. Vats, F. Su, R. J. Lonigro, X. Cao, S. Kalyana-Sundaram, R. Wang, Y. Ning, L. Hodges, A. Gursky, J. Siddiqui, S. A. Tomlins, S. Roychowdhury, K. J. Pienta, S. Y. Kim, J. S. Roberts, J. M. Rae, C. H. Van Poznak, D. F. Hayes, R. Chugh, L. P. Kunju, M. Talpaz, A. F. Schott, A. M. Chinnaiyan, Activating *ESR1* mutations in hormone-resistant metastatic breast cancer. *Nat. Genet.* **45**, 1446–1451 (2013).
11. R. Jeselsohn, R. Yelensky, G. Buchwalter, G. Frampton, F. Meric-Bernstam, A. M. Gonzalez-Angulo, J. Ferrer-Lozano, J. A. Perez-Fidalgo, M. Cristofanilli, H. Gómez, C. L. Arteaga, J. Giltnane, J. M. Balko, M. T. Cronin, M. Jarosz, J. Sun, M. Hawryluk, D. Lipson, G. Otto, J. S. Ross, A. Dvir, L. Soussan-Gutman, I. Wolf, T. Rubinek, L. Gilmore, S. Schnitt, S. E. Come, L. Pusztai, P. Stephens, M. Brown, V. A. Miller, Emergence of constitutively active estrogen receptor-α mutations in pretreated advanced estrogen receptor–positive breast cancer. *Clin. Cancer Res.* **20**, 1757–1767 (2014).
12. Cancer Genome Atlas Network, Comprehensive molecular portraits of human breast tumours. *Nature* **490**, 61–70 (2012).
13. D. Sefrioui, A. Perdrix, N. Sarafan-Vasseur, C. Dolfus, A. Dujon, J.-M. Picquenot, J. Delacour, M. Cornic, E. Bohers, M. Leheurteur, O. Rigal, I. Tennevet, J.-C. Thery, C. Alexandru, C. Guillemet, C. Moldovan, C. Veyret, T. Frebourg, F. Di Fiore, F. Clatot, Short report: Monitoring *ESR1* mutations by circulating tumor DNA in aromatase inhibitor resistant metastatic breast cancer. *Int. J. Cancer* **137**, 2513–2519 (2015).
14. D. S. Guttery, K. Page, A. Hills, L. Woodley, S. D. Marchese, B. Rghebi, R. K. Hastings, J. Luo, J. H. Pringle, J. Stebbing, R. C. Coombes, S. Ali, J. A. Shaw, Noninvasive detection of activating estrogen receptor 1 (*ESR1*) mutations in estrogen receptor–positive metastatic breast cancer. *Clin. Chem.* **61**, 974–982 (2015).
15. G. Siravegna, B. Mussolin, M. Buscarino, G. Corti, A. Cassingena, G. Crisafulli, A. Ponzetti, C. Cremolini, A. Amatu, C. Lauricella, S. Lamba, S. Hobor, A. Avallone, E. Valtorta, G. Rospo, E. Medico, V. Motta, C. Antoniotti, F. Tatangelo, B. Bellosillo, S. Veronese, A. Budillon, C. Montagut, P. Racca, S. Marsoni, A. Falcone, R. B. Corcoran, F. Di Nicolantonio, F. Loupakis, S. Siena, A. Sartore-Bianchi, A. Bardelli, Clonal evolution and resistance to EGFR blockade in the blood of colorectal cancer patients. *Nat. Med.* **21**, 795–801 (2015).
16. H. Weedon-Fekjær, B. H. Lindqvist, L. J. Vatten, O. O. Aalen, S. Tretli, Breast cancer tumor growth estimated through mammography screening data. *Breast Cancer Res.* **10**, R41 (2008).
17. E. C. de Bruin, N. McGranahan, R. Mitter, M. Salm, D. C. Wedge, L. Yates, M. Jamal-Hanjani, S. Shafi, N. Murugaesu, A. J. Rowan, E. Grönroos, M. A. Muhammad, S. Horswell, M. Gerlinger, I. Varela, D. Jones, J. Marshall, T. Voet, P. Van Loo, D. M. Rassl, R. C. Rintoul, S. M. Janes, S.-M. Lee, M. Forster, T. Ahmad, D. Lawrence, M. Falzon, A. Capitanio, T. T. Harkins, C. C. Lee, W. Tom, E. Teefe, S.-C. Chen, S. Begum, A. Rabinowitz, B. Phillimore, B. Spencer-Dene, G. Stamp, Z. Szallasi, N. Matthews, A. Stewart, P. Campbell, C. Swanton, Spatial and temporal diversity in genomic instability processes defines lung cancer evolution. *Science* **346**, 251–256 (2014).
18. M. Arnedos, S. Drury, M. Afentakis, R. A'Hern, M. Hills, J. Salter, I. E. Smith, J. S. Reis-Filho, M. Dowsett, Biomarker changes associated with the development of resistance to aromatase inhibitors (AIs) in estrogen receptor-positive breast cancer. *Ann. Oncol.* **25**, 605–610 (2014).
19. V. Taly, D. Pekin, L. Benhaim, S. K. Kotsopoulos, D. Le Corre, X. Li, I. Atochin, D. R. Link, A. D. Griffiths, K. Pallier, H. Blons, O. Bouché, B. Landi, J. B. Hutchison, P. Laurent-Puig, Multiplex picodroplet digital PCR to detect *KRAS* mutations in circulating DNA from the plasma of colorectal cancer patients. *Clin. Chem.* **59**, 1722–1731 (2013).
20. E. López-Knowles, C. V. Segal, Q. Gao, I. Garcia-Murillas, N. C. Turner, I. Smith, L.-A. Martin, M. Dowsett, Relationship of *PIK3CA* mutation and pathway activity with antiproliferative response to aromatase inhibition. *Breast Cancer Res.* **16**, R68 (2014).
21. H. Li, B. Handsaker, A. Wysoker, T. Fennell, J. Ruan, N. Homer, G. Marth, G. Abecasis, R. Durbin; 1000 Genome Project Data Processing Subgroup, The Sequence Alignment/Map format and SAMtools. *Bioinformatics* **25**, 2078–2079 (2009).

Acknowledgments: We thank N. Orr, K. Tomczyk, D. Novo, and F. Daley for technical assistance. **Funding:** This research was funded by National Health Service funding to the NIHR Biomedical Research Centre at The Royal Marsden and the Institute of Cancer Research, Cancer Research UK C30746/A16642, Breast Cancer Now with support from the Mary-Jean Mitchell Green Foundation, the Cridlan Trust, and the Susan G. Komen Foundation. **Author contributions:** G.S. and N.C.T. designed the study and set up the database. G.S., I.E.S., and N.C.T. enrolled the patients. R.R., L.-A.M., and M.D. selected and collected the samples for the validation cohort. G.S., S.H., and I.G.-M. designed the assays. G.S., S.H., I.G.-M., A.P., N.T., A.N., P.O., and E.-L.K. conducted the experiments. G.S., S.H., S.C., and I.G.-M. analyzed the data and G.S. and N.C.T. did the statistical analyses. K.F. and I.K. performed the next-generation sequencing (NGS) experiment. R.J.C. performed the NGS analysis. G.S., I.G.-M., and N.C.T. wrote the manuscript with assistance and final approval from all authors. **Competing interests:** N.C.T. has received advisory board honoraria from Roche/Genentech and AstraZeneca. M.D. is on the scientific advisory board of Radius and has paid consulting relationships with GTx, Roche/Genentech, Genoptix, NanoString, Pfizer, GlaxoSmithKline, AstraZeneca, and Ventana. All other authors declare that they have no competing interests.

Submitted 8 June 2015
Accepted 29 September 2015
Published 11 November 2015
10.1126/scitranslmed.aac7551

Citation: G. Schiavon, S. Hrebien, I. Garcia-Murillas, R. J. Cutts, A. Pearson, N. Tarazona, K. Fenwick, I. Kozarewa, E. Lopez-Knowles, R. Ribas, A. Nerurkar, P. Osin, S. Chandarlapaty, L.-A. Martin, M. Dowsett, I. E. Smith, N. C. Turner, Analysis of *ESR1* mutation in circulating tumor DNA demonstrates evolution during therapy for metastatic breast cancer. *Sci. Transl. Med.* **7**, 313ra182 (2015).

Analysis of *ESR1* mutation in circulating tumor DNA demonstrates evolution during therapy for metastatic breast cancer

Gaia Schiavon, Sarah Hrebien, Isaac Garcia-Murillas, Rosalind J. Cutts, Alex Pearson, Noelia Tarazona, Kerry Fenwick, Iwanka Kozarewa, Elena Lopez-Knowles, Ricardo Ribas, Ashutosh Nerurkar, Peter Osin, Sarat Chandarlapaty, Lesley-Ann Martin, Mitch Dowsett, Ian E. Smith and Nicholas C. Turner (November 11, 2015)

Science Translational Medicine **7** (313), 313ra182. [doi: 10.1126/scitranslmed.aac7551]

Editor's Summary

An evolving problem

A large number of breast cancers express the estrogen receptor, making them susceptible to hormonal treatments. Unfortunately, these tumors can develop mutations in the estrogen receptor gene (*ESR1*) and become resistant to hormonal therapies that were previously effective. Schiavon *et al*. used three independent cohorts of breast cancer patients to demonstrate that these mutations only evolved in cases where hormonal therapy was started late in the course of the disease, after development of metastasis, and not during the initial course of treatment. If these findings are confirmed in prospective clinical trials, then they will explain why starting hormonal treatment early decreases the risk of subsequent resistance to hormonal therapy.